THE JOURNAL OF BIOLOGICAL CHEMISTRY VOL. 284, NO. 31, pp. 20840–20847, July 31, 2009

Cab45b, a Munc18b-interacting Partner, Regulates Exocytosis in Pancreatic β-Cells*

Received for publication, March 9, 2009, and in revised form, May 5, 2009 Published, JBC Papers in Press, June 1, 2009, DOI 10.1074/jbc.M109.017467

Yi Zhang[‡], You-hou Kang[‡], Nathan Chang[‡], Patrick P. L. Lam[‡], Yunfeng Liu[‡], Vesa M. Olkkonen[§], and Herbert Y. Gaisano[‡1]

From the [‡]Departments of Medicine and Physiology, University of Toronto, Toronto, Ontario M5S 1A8, Canada and the [§]National Institute for Health and Welfare and Institute for Molecular Medicine Finland (FIMM), University of Helsinki, Biomedicum, P. O. Box 104, FI-00251 Helsinki, Finland

Cab45b is a cytosolic Ca^{2+}-binding protein reported to regulate zymogen secretion in pancreatic acini. We now show that Cab45b is also expressed in pancreatic islet β-cells and interacts there with the Sec1-Munc18 protein Munc18b. We employed patch clamp cell capacitance measurements to show that antibodies against Cab45b inhibited depolarization-evoked membrane capacitance increments, suggesting an impact on β-cell granule exocytosis, both the readily releasable granule pool and refilling of this pool. Site-specific mutants in the Cab45b EF-hands were used to dissect the molecular interactions involved in Cab45b function. Mutants in EF-hands 2 and 3 had no detectable effects on interaction of Cab45b with Munc18b and did not affect the depolarization-evoked calcium currents, but remarkably, they facilitated the complex formation of Munc18b with syntaxin-2 and -3. As a result, these two EF-hand mutants inhibited β-cell membrane capacitance increments. This inhibition is mediated via Munc18b because Munc18b silencing with small interfering RNA abolished the effects of these two mutants. The results suggest a mechanism for Cab45b action that involves regulating the dynamic association of Munc18b with SNAREs to impact β-cell granule exocytosis.

It is well established that the soluble *N*-ethylmaleimide-sensitive factor attachment protein receptor (SNARE)[2] proteins form the core machinery responsible for the fusion of transport vesicles, including secretory granules, with their target membranes. A number of accessory factors regulate SNARE function in membrane fusion (1). The Sec1-Munc18 (SM) proteins constitute a family of central SNARE regulators that bind syntaxins to influence secretory vesicle docking and fusion directly (2, 3). In mammals, there are seven SM proteins, of which the Munc18 isoforms a, b, and c are involved in exocytosis at the plasma membrane (4, 5). The Munc18 proteins were initially proposed to function as negative regulators of membrane fusion by inhibiting the assembly of *trans*-SNARE complexes. However, recent studies suggest that the Munc18 proteins regulate the transition of syntaxin from closed to open conformation, thereby facilitating SNARE complex assembly (6, 7).

A number of non-syntaxin-binding partners of the SM proteins have been identified and are suggested to modulate the SM protein-syntaxin interactions (8–11). Recently, we reported a novel SM-binding protein, a cytosolic splice variant of the EF-hand Ca^{2+}-binding protein Cab45 (designated Cab45b) expressed in pancreatic acini. Cab45b binds to Munc18b in complex with syntaxin-2 (Syn-2) and -3 (Syn-3) and directly influences amylase release from acini (12). Munc18b is thought to control secretory functions in non-neuronal cells, such as epithelial cells (13–15), pancreatic acinar cells (12), mast cells (16), and kidney medullary cells (17), whereas no function in neuronal or neuroendocrine cells has been assigned to this protein. In this study, we demonstrate that Cab45b is expressed in the neuroendocrine pancreatic islet β-cells and is associated with Munc18b-Syn-2 and Munc18b-Syn-3 complexes. Using cell membrane capacitance measurement, a well established technique for monitoring exocytosis in neurons and neuroendocrine cells (18, 19), we further dissect the functional domains within Cab45b (EF-hands 2 and 3) that impact the association of Munc18b with syntaxins to influence insulin granule exocytosis.

EXPERIMENTAL PROCEDURES

Expression Plasmids and Recombinant GST Fusion Proteins—The constructs pGEX1λT-Cab45b-WT, -mEF1 (mutant EF-hand 1, E25Q), -mEF2 (E70Q), and -mEF3 (E106Q) were generated as we reported previously (12). GST fusion proteins were expressed in *Escherichia coli* and purified on glutathione-Sepharose following the manufacturer's instructions (Amersham Biosciences).

Islet Isolation and Cell Culture—Rat islets were isolated by collagenase digestion from male Sprague-Dawley rats weighing 250–350 g and separated by density gradient centrifugation, as described previously (20). Animal procedures were performed in accordance with the University of Toronto Animal Care Committee ethical guidelines. To obtain single islet cells, the intact rat islets were dispersed in dispase II solution (Roche Applied Science) at 37 °C for 5 min, and the single cells were placed on glass coverslips. The dispersed islet cells were cultured in RPMI 1640 medium containing 11.1 mM glucose supplemented with 10% fetal bovine serum, 10 mM HEPES, 100

* This work was supported by Canadian Institutes for Health Research Grant MOP 89889.

[1] To whom correspondence should be addressed: Dept. of Medicine, University of Toronto, Rm. 7226 Medical Sciences Bldg., Toronto, Ontario M5S 1A8, Canada. Tel.: 416-978-1526; Fax: 416-978-8765; E-mail: herbert.gaisano@utoronto.ca.

[2] The abbreviations used are: SNARE, soluble *N*-ethylmaleimide-sensitive factor attachment protein receptor; F, farad(s); GST, glutathione *S*-transferase; RRP, readily releasable granule pool; siRNA, small interfering RNA; SM, Sec1-Munc18; Syn, syntaxin; WT, wild type.

units/ml penicillin, and 100 μg/ml streptomycin for 24–72 h before experiments.

Confocal Immunofluorescence Microscopy—Dispersed single islet cells were costained for Cab45b and either insulin or glucagon, and some islet cells were costained for insulin and Munc18b. Briefly, cells were placed on glass coverslips, fixed with 2% paraformaldehyde, and rinsed in phosphate-buffered saline for 5 min. The cells were then treated with 0.1% Triton X-100 in phosphate-buffered saline for 15 min, washed, and then treated with 10% normal goat serum in phosphate-buffered saline for 1 h at 25 °C. After the wash, the cells were incubated with two of the following primary antibodies: rabbit anti-Cab45b (1:100; prepared in the Olkkonen laboratory), guinea pig anti-insulin (1:200; Sigma), mouse anti-glucagon (1:200; Sigma), and rabbit anti-Munc18b (1:100; prepared in the Olkkonen laboratory) for 1 h at the indicated dilution, followed by the appropriate fluorescein isothiocyanate- or Texas Red-conjugated secondary antiserum (1 h at 25 °C). The specimens were mounted in glycerol and examined using an LSM510 laser scanning confocal imaging system (Carl Zeiss, Oberkochen, Germany).

Electrophysiology—Cells were patch-clamped in conventional whole-cell configuration at 33–34 °C. Islet β-cells were identified by cell size (>4 pF) and by their Na^+ current inactivation properties as described previously (21). Experiments were performed using an EPC-9 amplifier and PULSE software from HEKA Electronik (Lambrecht, Germany) as we have described (22). Patch pipettes had typical resistances of 3–6 megaohms when fire-polished and filled with an intracellular solution containing 120 mM CsCl, 20 mM tetraethylammonium chloride, 1 mM $MgCl_2$, 0.05 mM EGTA, 10 mM HEPES, 0.1 mM cAMP, and 5 mM MgATP, pH 7.3, with CsOH. The indicated antibodies or recombinant fusion proteins were added to the intracellular solution before experiments. After whole-cell configuration was established, the intracellular solution was dialyzed into the cell via patch pipette for 1 min, and then the cell membrane capacitance (C_m) or Ca^{2+} currents were measured. Extracellular solutions for capacitance measurements contained 118 mM NaCl, 20 mM tetraethylammonium chloride, 2.6 mM $CaCl_2$, 5 mM HEPES, 5.6 mM KCl, 1.2 mM $MgCl_2$, and 3 mM glucose, pH 7.4, with NaOH. In the recordings of depolarization-evoked Ca^{2+} currents, the following extracellular solution was used: 100 mM NaCl, 20 mM tetraethylammonium chloride, 20 mM $BaCl_2$, 5 mM HEPES, 4 mM CsCl, 1 mM $MgCl_2$, and 3 mM glucose, pH 7.4, with NaOH. Here, we employed Ba^{2+} to replace Ca^{2+} as the charge carrier to amplify Ca^{2+} current responses during the depolarization stimulus.

In Vitro Binding Assay and Western Blotting—Rat islets were lysed by sonication in binding buffer (25 mM HEPES, pH 7.5, 100 mM KCl, 1.5% Triton X-100, 2 μM pepstatin A, 1 μg/ml leupeptin, and 10 μg/ml aprotinin), and insoluble material was removed by centrifugation at 55,000 × *g* at 4 °C for 40 min. For binding assay, the detergent extract (0.5 ml, 2.0 μg/μl protein) of rat islets was incubated with GST (as a negative control), GST-Cab45b-WT, -mEF1, -mEF2, or -mEF3 (bound to glutathione-agarose, 400 pmol of protein each) at 4 °C for 2 h. The samples were then washed three times with washing buffer (20 mM HEPES, pH 7.4, 150 mM KoAc, 1 mM EDTA, 5% glycerol,

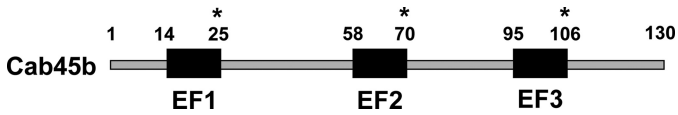

FIGURE 1. **Structure of Cab45b.** Cab45b consists of 130 amino acid residues and three EF-hand motifs (EF1, Asp^{14}–Glu^{25}; EF2, Asp^{58}–Glu^{70}; and EF3, Asp^{95}–Glu^{106}). *Numbers* indicate amino acid positions. Point mutations in the EF-hands are indicated with *asterisks*.

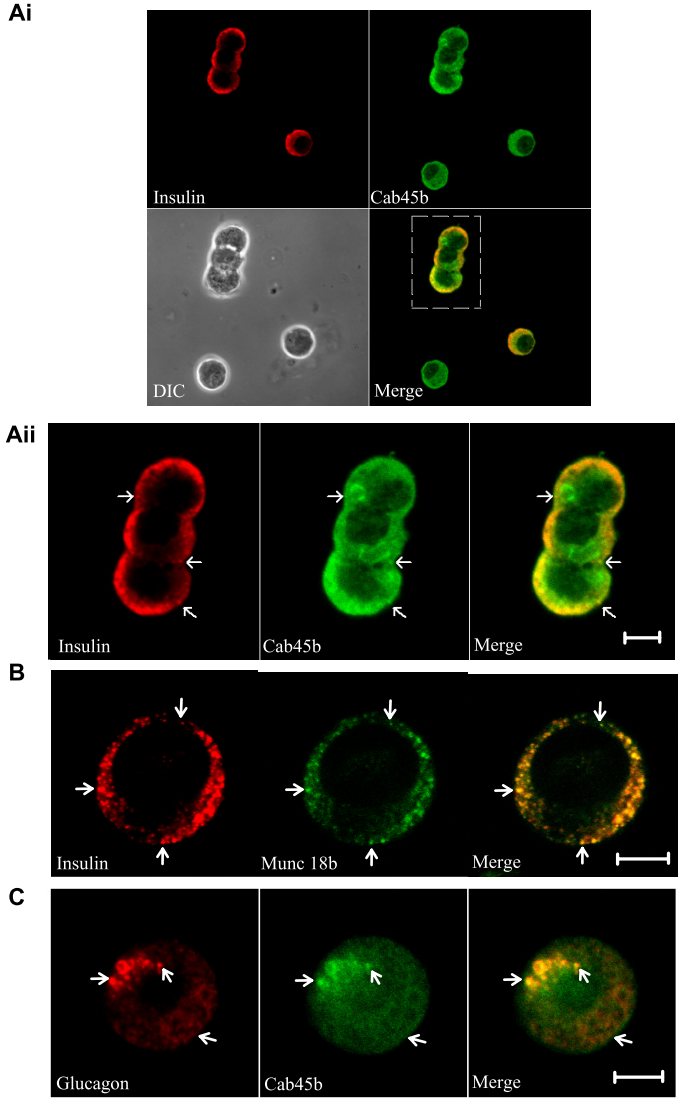

FIGURE 2. **Cab45b is present in rat pancreatic islet cells.** *Ai*, representative confocal micrographs of dispersed rat islet cells were costained for insulin and Cab45b. Note that a non-insulin-staining cell is also positive for Cab45b. *DIC*, differential interference contrast. *Aii*, the high-power magnification of *Ai* shows the localization of insulin and Cab45b in rat β-cells. *B*, representative confocal images show the distribution of insulin and Munc18b in rat β-cells. *C*, a representative confocal image shows that Cab45b is present in islet α-cells identified by staining for glucagon. *Arrows* indicate the granules. *Scale bars*, 5 μm. The images shown represent three independent experiments for each of the coimmunostainings.

and 0.1% Triton X-100), separated on 12% SDS-PAGE, and transferred to nitrocellulose membrane. The precipitated and separated proteins were identified with specific antibodies, including mouse anti-Munc18a (1:1000; Transduction Laboratories, Lexington, KY), rabbit anti-Munc18b (1:500) (13, 14), rabbit anti-Munc18c (1:800; a gift from Y. Tamori, Kobe University, Kobe, Japan), mouse monoclonal anti-Syn-1A (1:1000;

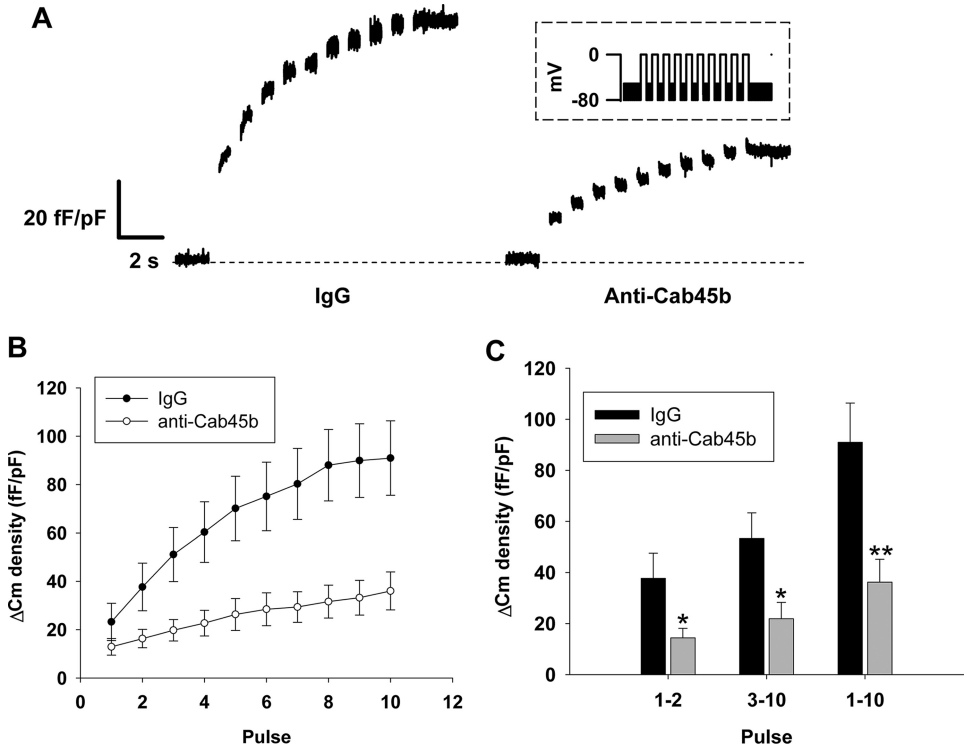

FIGURE 3. **Anti-Cab45b antibodies inhibit exocytosis in rat pancreatic islet β-cells.** A train of ten 500-ms depolarizations from −70 to 0 mV was applied to rat β-cells, and ΔC_m values were measured. ΔC_m density (in femtofarads/picofarads) is the capacitance change normalized for cell size. *A*, representative capacitance traces recorded from β-cells treated with control IgG (100 μg/ml) or anti-Cab45b (100 μg/ml). The *inset* shows the electrical depolarization protocol. *B*, summary of the cumulative increases in cell capacitance for each depolarizing pulse. *C*, summary of ΔC_m evoked by the first 2 pulses ($pulse_{1-2}$), the last 8 pulses ($pulse_{3-10}$), and all of the 10 depolarization pulses ($pulse_{1-10}$). The data shown represent the mean ± S.E. from three independent experiments; each experiment included two to three cells for each group (total n = seven cells for IgG control, n = eight cells for anti-Cab45b group).*, $p < 0.05$; **, $p < 0.01$, compared with the IgG control.

Sigma), rabbit anti-Syn-2 and -Syn-3 (affinity-purified) and anti-Syn-4 (1:1000; Synaptic System, Goettingen, Germany), or mouse soluble SNAP-25 (1:1000; Sternberger Monoclonals, Baltimore, MD). To examine whether Cab45b-mEF3 is able to bind directly to Munc18b but not Syn-3, HEK293 cells were infected with Ad-Munc18b, and BHK-21 cells were transfected with pcDNA3-Syn-3. GST-Cab45b-mEF1 (as negative control) and -mEF3 (400 or 800 pmol of protein) were used to precipitate Munc18b and Syn-3 from Munc18b- and Syn-3-expressing cell lysate extracts (650 μg of protein), respectively.

Small Interfering RNA (siRNA) Transfection—siRNAs were purchased from Invitrogen. The sequences of siRNA against Munc18b are as follows: sense, 5′-GCC CUG AUU GCG GAC UUC CAG GGA A-3′; and antisense, 5′-UUC CCU GGA AGU CCG CAA UCA GGG C-3′. For the negative control, scrambled siRNA (sense, 5′-CGG UUU GGG UGU GCA GUA CAA ACA G-3′; and antisense, 5′-CUG UUU GUA CUG CAC ACC CAA ACC G-3′) was used. INS-1E cells (gift from C. Wollheim) were used for siRNA (25 nM) transfection using Lipofectamine RNAiMAX (Invitrogen). A transfection efficiency of 85–90% was observed at 48 h, and then the cells were patch-clamped for capacitance measurements.

Statistical Analysis—All data are presented as means ± S.E. Statistical analysis was done by Student's *t* test, and significance was assumed at $p < 0.05$ by using the software SigmaPlot (SigmaPlot 2001, SPSS Science). Patch clamp data were analyzed with IGOR Pro 3.12 software (Wavemetrics, Lake Oswego, OR). The integrated Ca^{2+} currents during the depolarizations were determined by the software PULSEFIT (HEKA Electronik).

RESULTS

Cab45b Is Present in Neuroendocrine Pancreatic Islet β- and α-Cells—Cab45 is a 42-kDa EF-hand Ca^{2+}-binding protein that localizes to the Golgi lumen (23, 24). The recently discovered short splice variant Cab45b (15 kDa) consists of 130 amino acid residues and three EF-hand motifs (Fig. 1) (12). Confocal immunofluorescence microscopy analysis of rat islet cells using an affinity-purified anti-Cab45b antibody revealed strong staining of the β-cells identified by costaining for insulin (Fig. 2*Ai*). The Cab45b fluorescence showed in part an even, cytosolic-appearing distribution, but more intense fluorescence was observed in the peripheral region in proximity of the plasma membrane, where also most of the insulin-positive granules are localized (Fig. 2*Aii*). In this region, the Cab45b and insulin signals colocalized substantially. In the β-cells, Munc18b displayed a prominent insulin granule localization (Fig. 2*B*), consistent with the notion that it may recruit part of the Cab45b on granule membranes. Cab45b was also detected in the islet α-cells identified by staining for glucagon (Fig. 2*C*). In these cells, Cab45b was distributed between a cytosolic-appearing pattern and localization on the surface of glucagon granules.

Cab45b Controls Granule Exocytosis in Rat Pancreatic β-Cells—To address the functional role of endogenous Cab45b in β-cells, we employed patch clamp cell capacitance measurements as a surrogate marker for β-cell exocytosis. Experiments were conducted in the presence of nonimmune rabbit IgG (100 μg/ml) as a negative control or affinity-purified antibodies against Cab45b (100 μg/ml). We observed that the depolarization-evoked capacitance change (ΔC_m) was severely reduced in cells treated with anti-Cab45b compared with the IgG control (Fig. 3*A*). The total membrane ΔC_m in IgG-treated control cells was 91 ± 15 fF/pF (Fig. 3, *B* and *C*) in response to a train of 10 depolarizations ($pulse_{1-10}$). Under the same conditions, cells treated with anti-Cab45b demonstrated markedly weaker capacitance responses (36 ± 9 fF/pF, $p < 0.01$ *versus* control) (Fig. 3, *B* and *C*, $pulse_{1-10}$). These data suggest that Cab45b plays an important role in regulating β-cell exocytosis. The ΔC_m elicited by the first two depolarizations is thought to approximate the capacity of the readily releasable granule pool (RRP), whereas ΔC_m evoked by the subsequent depolarizations

estimates the refilling of the RRP by mobilization of new granules from the reserve pool (18, 19, 22, 25). Close inspection of the capacitance changes in this study revealed that the ΔC_m elicited by the first two depolarizations ($pulse_{1-2}$) in the cells treated with anti-Cab45b was 14 ± 4 fF/pF, markedly smaller than that in control cells (38 ± 10 fF/pF; $p < 0.05$) (Fig. 3*C*). A similar trend in the ΔC_m elicited by the last eight depolarizations ($pulse_{3-10}$) was observed (53 ± 10 fF/pF for control *versus* 22 ± 6 fF/pF for Cab45b; $p < 0.05$) (Fig. 3*C*). These results suggest that Cab45b may regulate both the β-cell RRP size and the refilling process of the RRP.

Structural Determinants in Cab45b That Impact Munc18b-Syntaxin Complex Formation—To identify structural determinants in Cab45b that might impact granule exocytosis in rat islet β-cells, we examined in patch clamp experiments the actions of full-length WT Cab45b and point mutations that inactivate each of the EF-hand domains, EF-hands 1 (E25Q, denoted mEF1), 2 (E70Q, denoted mEF2), and 3 (E106Q, denoted mEF3). We first examined the ability of each of these Cab45b proteins to associate with Munc18 and islet SNARE proteins. GST (as negative control) and GST-Cab45b-WT, -mEF1, -mEF2, and -mEF3 were used to pull down the proteins of interest in rat islet lysates, and the proteins associated with Cab45b were identified with specific antibodies. Cab45b-WT, -mEF1, -mEF2, and -mEF3 proteins were equally capable of pulling down Munc18b (Fig. 4*Ai*), indicating that the inactivating mutations within the EF domains did not block Cab45b binding to Munc18b. The Cab45b proteins did not pull down Munc18a or Munc18c (data not shown), supporting the view that Cab45b interacts specifically with the Munc18b isoform (12). Syn-4, which would have bound Munc18c (26), was likewise not coprecipitated. We then examined the syntaxins coprecipitated with the Munc18b-Cab45b complex. Cab45b-WT, -mEF1, -mEF2, and -mEF3 proteins were equally capable of pulling down Syn-1A (Fig. 4*Ai*) in pancreatic β-cells, indicating that the inactivating mutations within the EF domains did not interfere with the interaction of Syn-1A with Munc18b. Munc18b had previously been shown also to bind Syn-1A (27). However, Munc18b in complex with GST-Cab45b-mEF2 or -mEF3, but not GST-Cab45b-WT or -mEF1, pulled down Syn-2 and Syn-3, but not Syn-4 (Fig. 4*Ai*). The results suggest that Cab45b regulates the association of Munc18b with Syn-2 and Syn-3, thus controlling the participation of these syntaxins in SNARE complex assembly required for exocytosis. Of note, Cab45b-mEF3 in association with Munc18b formed a particularly abundant complex with Syn-3 and, to a lesser extent, also with Syn-2. In accordance with our previous observations (12), GST-Cab45b-mEF3 failed to pull down Syn-3 overexpressed in BHK-21 cells (Fig. 4*B*), a cell line that does not express Munc18b, but would pull down Munc18b overexpressed in HEK293 cells. Thus, there is no direct interaction between Cab45b and syntaxins. Therefore, these results suggest that Cab45b, particularly its EF3 domain, has a distinct function in regulating the interaction of Munc18b with Syn-2 and Syn-3. Distortion of the EF-hands 2 and 3 apparently facilitates the complex formation of the SM protein with Syn-2 and Syn-3 and could consequently influence SNARE complex assembly. Indeed, SNAP-25 was not pulled down by these GST-Cab45b

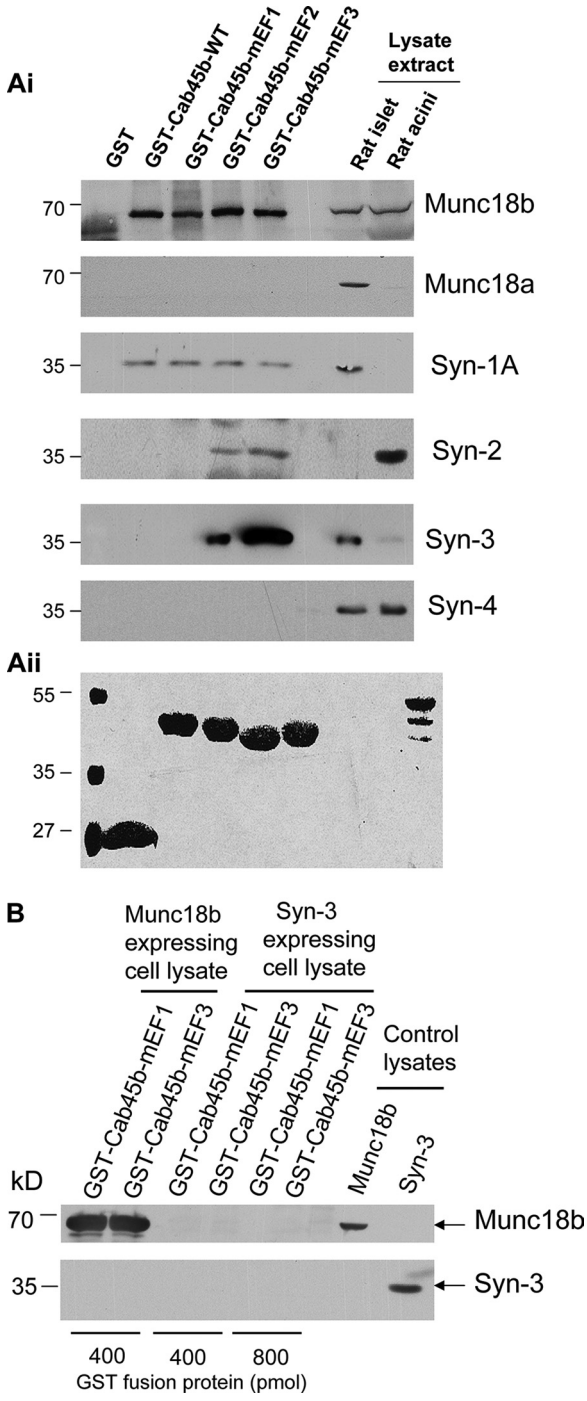

FIGURE 4. **Structural determinants in Cab45b that impact pancreatic islet Munc18b-syntaxin complexes.** *Ai*, *in vitro* binding assay with immobilized GST-Cab45b fusion proteins and Western blotting were performed as described under "Experimental Procedures." GST (negative control), GST-Cab45b-WT, or the EF-hand mutant proteins (GST-Cab45b-mEF1, -mEF2, and -mEF3) were used to perform pulldown from rat islet lysates (1000 μg of total protein), and the precipitates were Western-blotted with the indicated antibodies. Blots shown are representative of four separate experiments. Rat islet (15 μg of total protein) and rat acini (36 μg) are shown for a comparison. *Aii*, Ponceau S staining of the blot demonstrates the equal loading of the GST fusion proteins. *B*, both GST-Cab45b-mEF1 and -mEF3 are able to pull down Munc18b but not Syn-3 directly. HEK293 cells were infected with Ad-Munc18b, and BHK-21 cells were transfected with pBK-CMV-Syn-3. GST-Cab45b-mEF1 (as a negative control) and -mEF3 (400 or 800 pmol of protein, as indicated) were used to precipitate Munc18b and Syn-3 from Munc18b- and Syn-3-expressing cell lysate extracts (input, 650 μg of total protein), respectively. The total cell lysate extracts (25 μg of protein) are shown for a comparison.

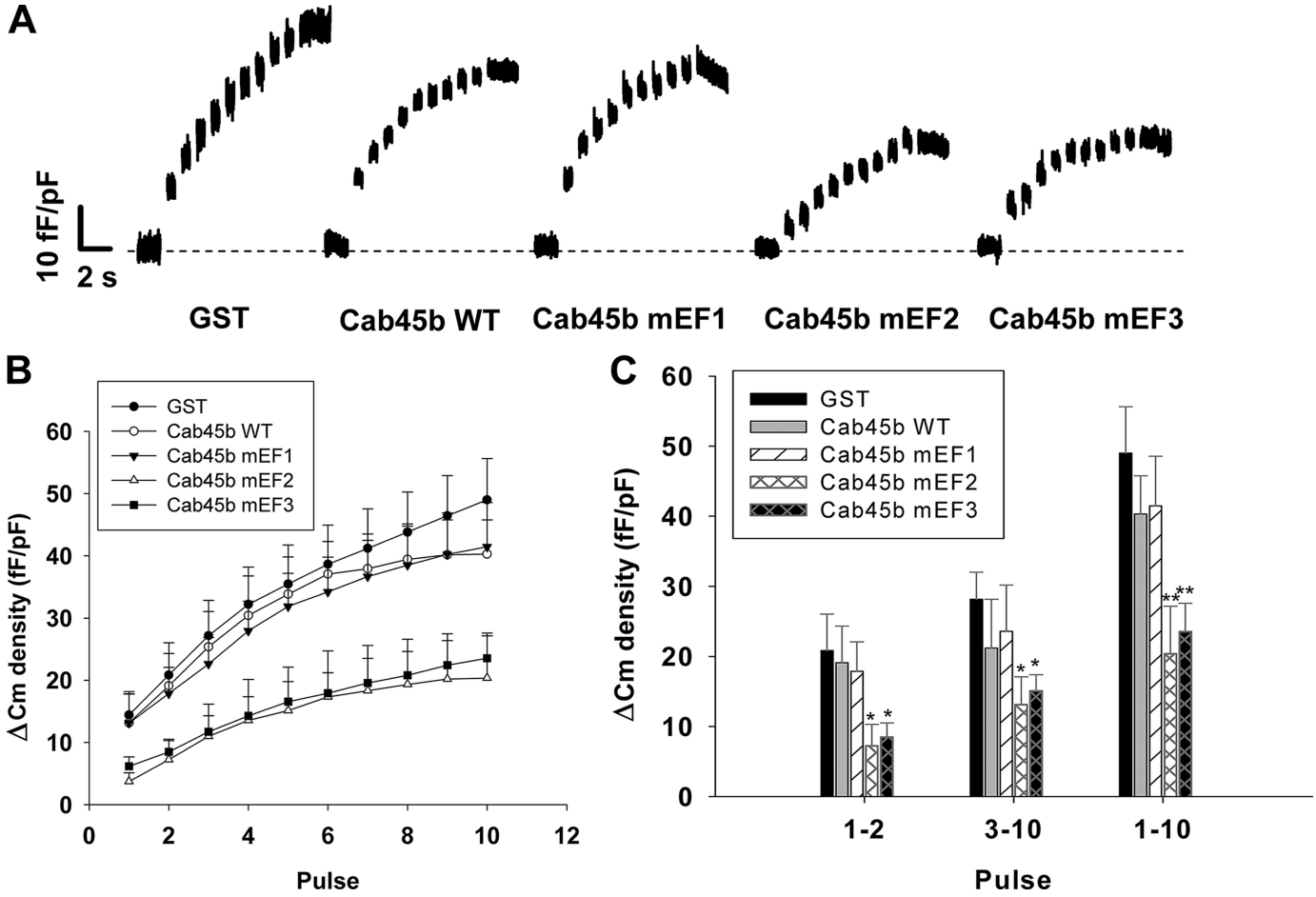

FIGURE 5. **Inactivation of Cab45b EF-hand 2 or -3 inhibits exocytosis in rat pancreatic β-cells.** The same stimuli as described in Fig. 3 were applied to rat β-cells to measure ΔC_m. *A*, representative capacitance traces recorded from the β-cells. Equal concentrations (1 μM) of GST (negative control), GST-Cab45b-WT, or mutant proteins (Cab45b-mEF1, -mEF2, and -mEF3) were dialyzed into the cells for 1 min, and the ΔC_m was measured. *B*, summary of cumulative increases in cell capacitance for each depolarizing pulse. *C*, summary of ΔC_m evoked by the first 2 pulses ($pulse_{1-2}$), the last 8 pulses ($pulse_{3-10}$), or all 10 of the depolarization pulses ($pulse_{1-10}$). The data shown represent mean ± S.E. from four independent experiments; each experiment included 2–3 cells for each group (total $n = 11$ cells for GST control, $n = 8$ cells for Cab45b-WT, $n = 11$ cells for Cab45b-mEF1, $n = 8$ cells for Cab45b-mEF2, $n = 10$ cells for Cab45b-mEF3). *, $p < 0.05$; **, $p < 0.01$, compared with the GST control.

complexes (data not shown), indicating that Syn-2 and Syn-3 bound to the Munc18b-Cab45b complexes are unable to form complexes with cognate SNARE partners such as SNAP-25.

Functional Domains within Cab45b Are Essential for Regulating Granule Exocytosis of Rat Pancreatic β-Cells—To examine whether these Cab45b structural requirements for binding Munc18b-syntaxin complexes are of functional significance, we performed capacitance measurements on rat islet β-cells dialyzed with each of the Cab45b-WT and -mEF proteins. Remarkably, the Cab45b-mEF2 and -mEF3 fusion proteins resulted in suppression of total ΔC_m ($pulse_{1-10}$) in β-cells ($p < 0.01$ *versus* GST control). Further analysis of the ΔC_m induced by the first two ($pulse_{1-2}$) or last eight ($pulse_{3-10}$) depolarizations revealed that both mEF2 and mEF3 profoundly inhibited the size of RRP and the refilling process of RRP, respectively (Fig. 5). In contrast, neither mEF1 nor Cab45b-WT caused any change of ΔC_m compared with the GST control (Fig. 5), indicating that a cellular excess of functionally normal Cab45b does not interfere with granule exocytosis.

Munc18b Is Essential in Mediating the Effects of Cab45b on Exocytosis—To confirm that Cab45b through its EF domains regulated exocytosis specifically by its actions on Munc18b, siRNA against Munc18b was employed on INS-1E cells to knock down the expression of endogenous Munc18b, and capacitance measurements were performed 48–72 h after transfection. The results showed that Munc18b siRNA greatly suppressed the endogenous level of Munc18b (Fig. 6*A*) and decreased the total ΔC_m compared with a scrambled control siRNA (Fig. 6, *B* and *C*). Of note, in the cells transfected with Munc18b siRNA, no differences were observed in total ΔC_m among groups treated with GST, Cab45b-WT, and Cab45b-mEF proteins (Fig. 6, *B* and *C*). These results indicate that genetic suppression of Munc18b abolishes the effects of Cab45b-mEF2 and -mEF3 on the capacitance changes, a surrogate marker for exocytosis. These results support our *in vitro* binding data and suggest that association with Munc18b is required for the interference of exocytosis by Cab45b-mEF2 and -mEF3.

Cab45b and Its Mutants Do Not Affect Depolarization-evoked Ca^{2+} Currents—Because ΔC_m is triggered by depolarization-evoked Ca^{2+} influx, we determined whether the Cab45b-WT or -mEF proteins might influence Ca^{2+} currents during the depolarization stimulus. As shown in Fig. 7, there were no significant differences in the integrated Ca^{2+}

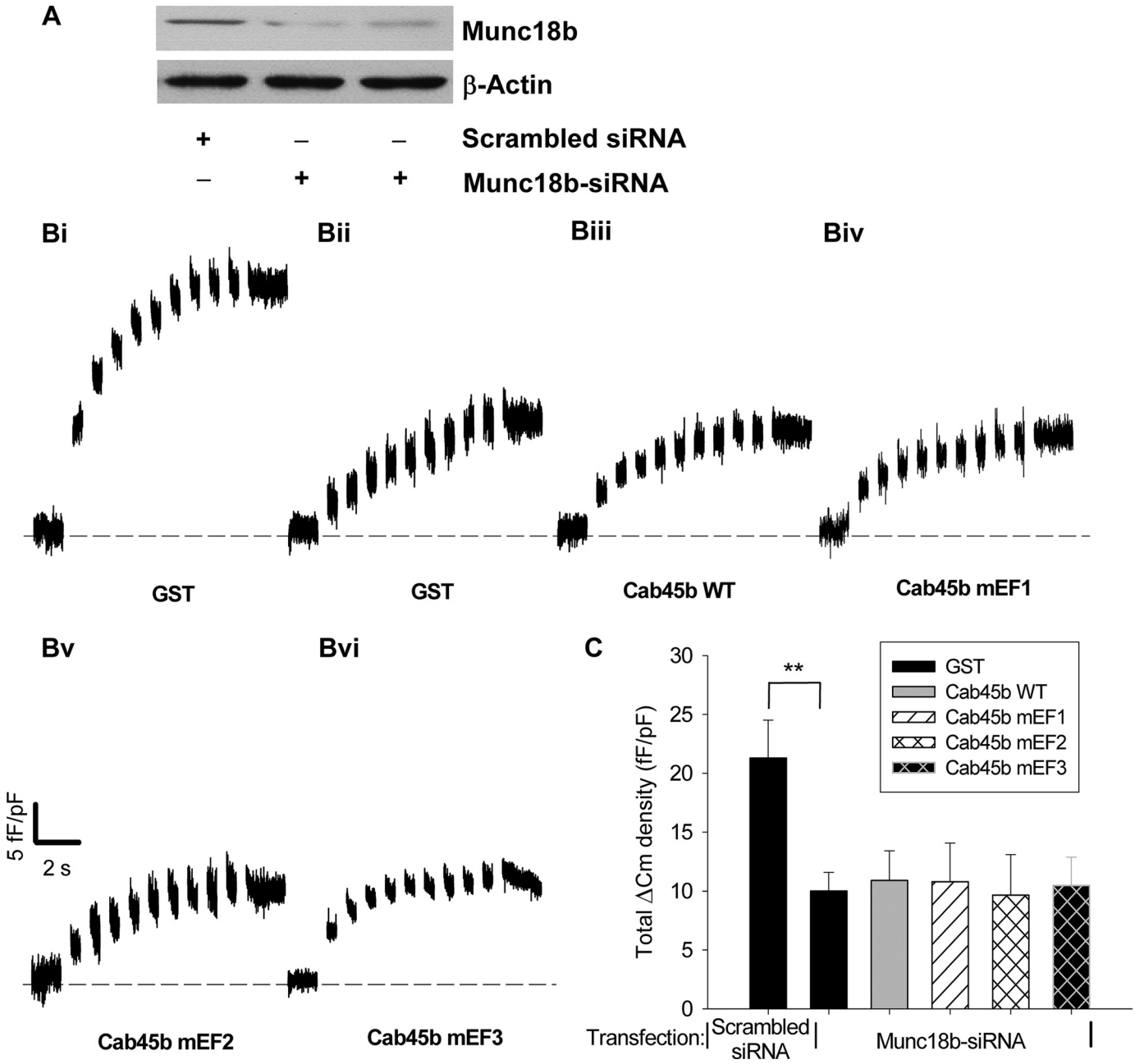

FIGURE 6. **siRNA suppression of endogenous Munc18b levels in INS-1E cells abolishes the effects of Cab45b-mEF2 and -mEF3 on exocytosis.** *A*, Western blot showing the effect of siRNA on Munc18b protein levels in INS-1E cells after a 48-h transfection with a scrambled siRNA or siRNA directed against Munc18b. Antibody against β-actin was used to verify equal loading of the lanes. *B*, representative capacitance traces recorded from INS-1E cells transfected with a scrambled siRNA (*Bi*) or Munc18b-siRNA (*Bii–Bvi*). Equal concentrations (1 μM) of GST, GST-Cab45b-WT, or mutant proteins (Cab45b-mEF1, -mEF2, and -mEF3) were dialyzed into the cells for 1 min, and the ΔC_m was measured. *C*, summary of total ΔC_m evoked by the 10 depolarization pulses ($pulse_{1-10}$). The data shown represent the mean ± S.E. from four independent experiments; each experiment included 2–3 cells for each group (total $n = 9$ cells for all groups except $n = 11$ for Cab45b-mEF3). **, $p < 0.01$, compared with the GST treatment from cells transfected with scrambled siRNA.

currents among groups treated with GST, Cab45b-WT, or Cab45b-mEF, indicating that the effects of Cab45b-mEF2 and -mEF3 on membrane capacitance changes were not caused by a change of Ca^{2+} influx but by the exocytotic machinery *per se*.

DISCUSSION

The present immunofluorescence analysis identified Cab45b in rat pancreatic islets, in both β- and α-cells. In β-cells, Cab45b, which is intrinsically cytosolic, was found concentrating in regions where the insulin granules are located. Furthermore, Munc18b was found prominently localized on the insulin granules. We have in this and a previous study (12) shown by GST pulldown and coimmunoprecipitation that Cab45b and Munc18b are physically associated in same protein complexes. Moreover, our findings using the yeast two-hybrid system (12) suggest a direct interaction of the two proteins. We therefore find it likely that Munc18b may interact with Cab45b on the

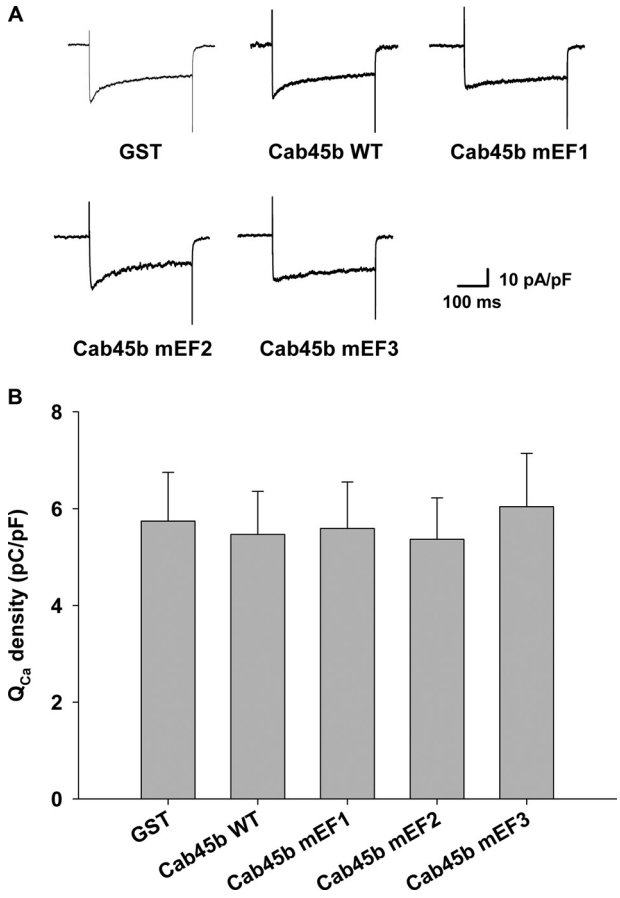

FIGURE 7. **Cab45b and its mutants do not affect Ca^{2+} currents in rat pancreatic β-cells.** *A*, representative Ca^{2+} currents evoked by a depolarization pulse from −70 to 0 mV. Equal concentrations (1 μM) of GST, GST-Cab45b-WT, or mutant proteins (Cab45b-mEF1, -mEF2, or -mEF3) were dialyzed into the cells for 1 min, and the current was measured. *B*, summary of integrated Ca^{2+} currents (Q_{Ca}) evoked by the depolarization pulses. The data shown represent the mean ± S.E. from four independent experiments; each experiment included 2–3 cells for each group (total $n = 10$ cells for GST control, Cab45b-WT, and Cab45b-mEF1, respectively; $n = 9$ for Cab45b-mEF2 and Cab45b-mEF3, respectively). No influence on Q_{Ca} was observed among these treatments.

surface of insulin granules. In this way, Cab45b is in a position to regulate the association of Munc18b with its cognate SNARE partners instrumental in membrane fusion in β-cells. The present data suggest that the actions of Cab45b profoundly influence the kinetics of insulin granule mobilization, priming, and release in pancreatic islet β-cells. Cab45b is capable of binding Munc18b but does not directly interact with syntaxins. Our results suggest that Cab45b regulates the association of Munc18b with Syn-2 and Syn-3, thus controlling the participation of these syntaxins in SNARE complex assembly required for exocytosis, which we measured using ΔC_m as a surrogate marker. This interpretation is supported by the fact that the Cab45b-mEF proteins inhibited capacitance increments but had no detectable effect on Ca^{2+} currents during depolarization stimulus.

We were able to pull down Syn-2 and Syn-3 only with the Cab45b-mEF2 and -mEF3 proteins and not with Cab45b-WT, suggesting that Munc18b complexes with syntaxins are of low abundance or unstable under steady-state conditions in the rat pancreatic islet, and the EF2 and -3 mutants most likely have a dominant interfering activity, possibly by causing sequestration of syntaxins in abnormally stable complexes with Munc18b. However, Munc18b-Cab45b-syntaxin complexes were readily coimmunoprecipitated from pancreatic acini (12), most likely reflecting a higher abundance or stability of such complexes in the acinar cells.

In neurons and neuroendocrine cells, research on exocytosis has focused mainly on the actions of Munc18a and Syn-1A (3, 28, 29). In fact, a recent report on a Syn-1A-deleted mutant showed reduction of docked insulin granules contributing to loss of glucose-stimulated first-phase insulin release (30). There is also evidence for the function of Munc18c and its cognate Q-SNARE partner Syn-4 in pancreatic β-cell insulin granule exocytosis (9, 10, 31, 32) contributing to second-phase insulin secretion (33, 34). Munc18b and its cognate Syn-2 and Syn-3, although present in neuroendocrine cells, have not been attributed a significant secretory role in these cells. In non-neuronal cells, Munc18b and its cognate SNAREs mediate not only fusion of secretory vesicles with the plasma membrane (14, 15, 17, 35), but also vesicle-vesicle fusion (16, 35, 36). Importantly, limited sequential vesicle-vesicle fusion also occurs in pancreatic islet β-cells (20, 37), and one can envision that Munc18b with its cognate syntaxin partners may play a role in such compound fusion events.

Cab45b or similar Cab45 variants present in neuroendocrine cells could facilitate the conversion of closed conformation Syn-2 and Syn-3 complexed with Munc18b to the open conformation capable of SNARE complex assembly required to influence their exocytotic functions. The secretory actions of Munc18b and its syntaxin partners may thus be enabled by Cab45b in both non-neuronal secretory (pancreatic acini (12) and neuroendocrine pancreatic islet β-cells. The role of Ca^{2+} binding by Cab45b is thus far unclear. It is obvious from previous work that Ca^{2+} is not required for the Munc18b-Cab45b interaction (12). Furthermore, even though the present study shows that mutating Cab45b EF-hands 2 and 3, which are important for calcium binding, does not inhibit the Munc18b-Cab45b interaction, it demonstrates the functional importance of the Ca^{2+}-binding EF-hands 2 and 3. We find it likely that these structural motifs, the conformation of which is putatively affected by bound Ca^{2+} ions, play a distinct role in controlling the interaction of Munc18b with syntaxins. This hypothesis will be addressed in detail in future studies.

Acknowledgment—We thank Pirjo Ranta for skilled technical assistance.

REFERENCES

1. Rothman, J. E. (2002) *Nat. Med.* **8,** 1059–1062
2. Toonen, R. F., and Verhage, M. (2003) *Trends Cell Biol.* **13,** 177–186
3. Gallwitz, D., and Jahn, R. (2003) *Trends Biochem. Sci.* **28,** 113–116
4. Garcia, E. P., Gatti, E., Butler, M., Burton, J., and De Camilli, P. (1994) *Proc. Natl. Acad. Sci. U.S.A.* **91,** 2003–2007
5. Tellam, J. T., McIntosh, S., and James, D. E. (1995) *J. Biol. Chem.* **270,** 5857–5863
6. Zilly, F. E., Sørensen, J. B., Jahn, R., and Lang, T. (2006) *PLoS Biol.* **4,** e330
7. Shen, J., Tareste, D. C., Paumet, F., Rothman, J. E., and Melia, T. J. (2007) *Cell* **128,** 183–195
8. Tsuboi, T., and Fukuda, M. (2006) *Mol. Biol. Cell* **17,** 2101–2112

9. Oh, E., Heise, C. J., English, J. M., Cobb, M. H., and Thurmond, D. C. (2007) *J. Biol. Chem.* **282,** 32613–32622
10. Ke, B., Oh, E., and Thurmond, D. C. (2007) *J. Biol. Chem.* **282,** 21786–21797
11. Okamoto, M., and Südhof, T. C. (1997) *J. Biol. Chem.* **272,** 31459–31464
12. Lam, P. P., Hyvärinen, K., Kauppi, M., Cosen-Binker, L., Laitinen, S., Keränen, S., Gaisano, H. Y., and Olkkonen, V. M. (2007) *Mol. Biol. Cell* **18,** 2473–2480
13. Riento, K., Jäntti, J., Jansson, S., Hielm, S., Lehtonen, E., Ehnholm, C., Keränen, S., and Olkkonen, V. M. (1996) *Eur. J. Biochem.* **239,** 638–646
14. Riento, K., Galli, T., Jansson, S., Ehnholm, C., Lehtonen, E., and Olkkonen, V. M. (1998) *J. Cell Sci.* **111,** 2681–2688
15. Riento, K., Kauppi, M., Keranen, S., and Olkkonen, V. M. (2000) *J. Biol. Chem.* **275,** 13476–13483
16. Martin-Verdeaux, S., Pombo, I., Iannascoli, B., Roa, M., Varin-Blank, N., Rivera, J., and Blank, U. (2003) *J. Cell Sci.* **116,** 325–334
17. Nicoletta, J. A., Ross, J. J., Li, G., Cheng, Q., Schwartz, J., Alexander, E. A., and Schwartz, J. H. (2004) *Am. J. Physiol. Cell Physiol.* **287,** C1366–C1374
18. Rorsman, P., and Renström, E. (2003) *Diabetologia* **46,** 1029–1045
19. Gillis, K. D., Mossner, R., and Neher, E. (1996) *Neuron* **16,** 1209–1220
20. Kwan, E. P., and Gaisano, H. Y. (2005) *Diabetes* **54,** 2734–2743
21. Göpel, S., Kanno, T., Barg, S., Galvanovskis, J., and Rorsman, P. (1999) *J. Physiol.* **521,** 717–728
22. Kwan, E. P., Xie, L., Sheu, L., Ohtsuka, T., and Gaisano, H. Y. (2007) *Diabetes* **56,** 2579–2588
23. Koivu, T., Laitinen, S., Riento, K., and Olkkonen, V. M. (1997) *DNA Seq.* **7,** 217–220
24. Scherer, P. E., Lederkremer, G. Z., Williams, S., Fogliano, M., Baldini, G., and Lodish, H. F. (1996) *J. Cell Biol.* **133,** 257–268
25. Gromada, J., Høy, M., Renström, E., Bokvist, K., Eliasson, L., Göpel, S., and Rorsman, P. (1999) *J. Physiol.* **518,** 745–759
26. Tellam, J. T., Macaulay, S. L., McIntosh, S., Hewish, D. R., Ward, C. W., and James, D. E. (1997) *J. Biol. Chem.* **272,** 6179–6186
27. Hata, Y., and Südhof, T. C. (1995) *J. Biol. Chem.* **270,** 13022–13028
28. Tomas, A., Meda, P., Regazzi, R., Pessin, J. E., and Halban, P. A. (2008) *Traffic* **9,** 813–832
29. Toonen, R. F., Kochubey, O., de Wit, H., Gulyas-Kovacs, A., Konijnenburg, B., Sørensen, J. B., Klingauf, J., and Verhage, M. (2006) *EMBO J.* **25,** 3725–3737
30. Ohara-Imaizumi, M., Fujiwara, T., Nakamichi, Y., Okamura, T., Akimoto, Y., Kawai, J., Matsushima, S., Kawakami, H., Watanabe, T., Akagawa, K., and Nagamatsu, S. (2007) *J. Cell Biol.* **177,** 695–705
31. Jewell, J. L., Luo, W., Oh, E., Wang, Z., and Thurmond, D. C. (2008) *J. Biol. Chem.* **283,** 10716–10726
32. Oh, E., Spurlin, B. A., Pessin, J. E., and Thurmond, D. C. (2005) *Diabetes* **54,** 638–647
33. Spurlin, B. A., and Thurmond, D. C. (2006) *Mol. Endocrinol.* **20,** 183–193
34. Oh, E., and Thurmond, D. C. (2009) *Diabetes* **58,** 1165–1174
35. Pickett, J. A., Thorn, P., and Edwardson, J. M. (2005) *J. Biol. Chem.* **280,** 1506–1511
36. Nemoto, T., Kimura, R., Ito, K., Tachikawa, A., Miyashita, Y., Iino, M., and Kasai, H. (2001) *Nat. Cell Biol.* **3,** 253–258
37. Takahashi, N., Hatakeyama, H., Okado, H., Miwa, A., Kishimoto, T., Kojima, T., Abe, T., and Kasai, H. (2004) *J. Cell Biol.* **165,** 255–262